J Polym Res (2016) 23: 172
DOI 10.1007/s10965-016-1073-7

ORIGINAL PAPER

Chemical oxidation polymerization and characterization of poly ortho-anisidine nanoparticles

Kiattipong Khamngoen[1] · **Nophawan Paradee**[1] · **Anuvat Sirivat**[1]

Received: 3 March 2016 / Accepted: 28 July 2016 / Published online: 2 August 2016

Abstract Poly *o*-anisidine (POA) is a conductive polymer that can conduct electrons by a π-conjugated system. POA is a derivative of polyaniline, however, it still exhibits low electrical conductivity. This work is focused on the improvement of electrical conductivity of POA by synthesizing POA in nanoparticle forms using an anion as a dopant. POA nanoparticles were obtained from chemical oxidation polymerization using an ammonium persulfate as an oxidant and a sodium dodecyl sulfate (SDS) as a surfactant for controlling POA size and shape. The properties of the POA nanoparticles were characterized by FT-IR, UV-Vis spectroscopy, TGA, and SEM. POA nanoparticles shapes were nanofibers with a diameter varying from 63 to 129 nm depending on the polymerization temperature, polymerization time, and SDS concentration. The electrical conductive obtained varied from 0.022 to 168 S/cm, a variation of 4 orders of magnitude, depending on the POA nanoparticle size and SDS concentration. The smallest POA nanoparticle size provided the highest electrical conductivity because of the larger surface area for electron transfer. Thus, this work demonstrated the extremely high electrical conductivity of the synthesized nanofiber shape POA which have not previously been reported elsewhere.

Keywords Poly *o*-anisidine · Conductive polymer · Chemical oxidation polymerization · Nanoparticle

✉ Anuvat Sirivat
anuvat.s@chula.ac.th

[1] The Petroleum and Petrochemical College, Chulalongkorn University, Bangkok 10330, Thailand

Introduction

Polymers are mostly used for insulator applications. Some polymers can be classified as semiconductors because of their electrical conductivity [1]. A conductive polymer allows the electron transfer because its structure consists of the conjugated bonds (alternating single and double bonds or conjugated segments coupled with atoms providing p-orbitals for a continuous orbital overlap) which provide electron mobility [2, 3]. Examples of conductive polymers are polyaniline [4], polypyrrole [5], and polyacetylene [6] (Table 1).

A conductive polymer doped by a chemical doping agent possesses charge defects (polaron, bipolaron, and soliton) in its structure through a doping process. These defects induce the charge to be stabilized on the polymer chain that can conduct electron [1]. The doping methods can be proceeded by chemical doping (partially oxidized or reduced by electron donors or electron accepters), electrochemical doping (applied DC power source) [7], photo–doping, charge-injection doping, and non–redox doping [1].

Poly *o*-anisidine (POA) is a one of conductive polymers, a derivative of aniline; it can be synthesized by the electrochemical and chemical oxidation polymerizations [8]. POA has been used as a biosensor [9], surface coating [10], gas separation [11], and etc. Nevertheless, POA exhibits poor electrical conductivity (10^{-3} - 10^{-4} S/cm) [12], this is the limitation for using POA in various electrical applications.

There have been numerous reports on the synthesis of conductive polymers with nano-structures to improve the electrical conductivity because the nano-structures increase accessible path ways for electrons transfer [13].

In this work, the synthesis of the nano–structure POA was carried out by chemical oxidation polymerization using sodium dodecyl sulfate (SDS) as a surfactant template. The synthesized POA was characterized by FT-IR, H-NMR, UV-vis,

Table 1 Comparison of particle size, particle shape, and electrical conductivity of POA obtained under various synthesis conditions

Synthesis method	Particle size (nm)	Shape	Electrical conductivity (S/cm)	Remarks*
Emulsion polymerization (SDS as surfactant)	-	Lamellar	$8.85 \pm 0.03 \times 10^{-2}$	OA:SDS = 1:0.008
	-	Lamellar	$1.66 \pm 0.01 \times 10^{-1}$	OA:SDS = 1:0.12
	90 ± 17.9	Fiber agglomerate	1.35 ± 0.03	OA:SDS = 1:1
	73 ± 13.1	Fiber agglomerate	9.05 ± 2.93	OA:SDS = 1:4
	73 ± 13.5	Fiber agglomerate	24.19 ± 1.07	OA:SDS = 1:6
	65 ± 8.6	Fully formed Fiber	168.96 ± 34.61	OA:SDS = 1:8
	80 ± 13.7	Fiber agglomerate	126.23 ± 2.24	OA:SDS = 1:10
	60 ± 11.2	Fiber agglomerate	8.66 ± 0.79	OA:SDS = 1:12
Chemical oxidation polymerization [40]	-	Spherical	$1.8 \pm 0.2 \times 10^{-3}$	OA:MSA = 1:1.25
	-	Plate-like	$8.4 \pm 0.8 \times 10^{-3}$	OA:pTSA =1:1.25
	-	Spherical	$2.5 \pm 0.1 \times 10^{-3}$	OA:HCl = 1:1.25
Emulsion polymerization (SDS as surfactant) [39]	40–50	rod-shaped	-	OA:SDS = 1:7.9

*Ratios given are mole ratios

and TGA to confirm POA structure. The effects of polymerization temperature, polymerization time, and surfactant concentration on the morphology and electrical conductivity of POA were investigated and shall be reported here.

Experimental

Materials

An *o*-anisidine, OA, (AR grade, Sigma-Aldrich) was used as a monomer. Ammonium persulfate, APS, (AR grade, Sigma-Aldrich), and hydrochloric acid, HCl, solution, 0.1 M (ACI Labscan) were used as an oxidant and a catalyst, respectively. Sodium dodecylsulfate, SDS, (AR grade, Loba Chemie) was used as a surfactant to control size of polymer particles. Deionized water, acetone (AR grade, ACI Labscan), and methanol (AR grade, QRëC) were used as solvents without further purification.

Synthesis of poly *o*-anisidne (POA)

POA was synthesized via a chemical oxidation polymerization [8]. APS, as an oxidizer (0.49 g), was dissolved in HCl solution (0.1 M, 10 ml). An *o*-anisidine 0.52 g (0.0043 M) and SDS were dissolved in the HCl solution (0.1 M, 100 ml) at various mole ratios (SDS / OA mole ratio) from 0.008 to 16. Then the APS solution was fed into the monomer solution at 1.0 ml/min. The monomer solution and the APS solution were mixed at 3, 25, and 60 °C for 18, 48, and 72 h. The product was terminated and precipitated with methanol. The dark green POA product was filtered and washed with methanol,

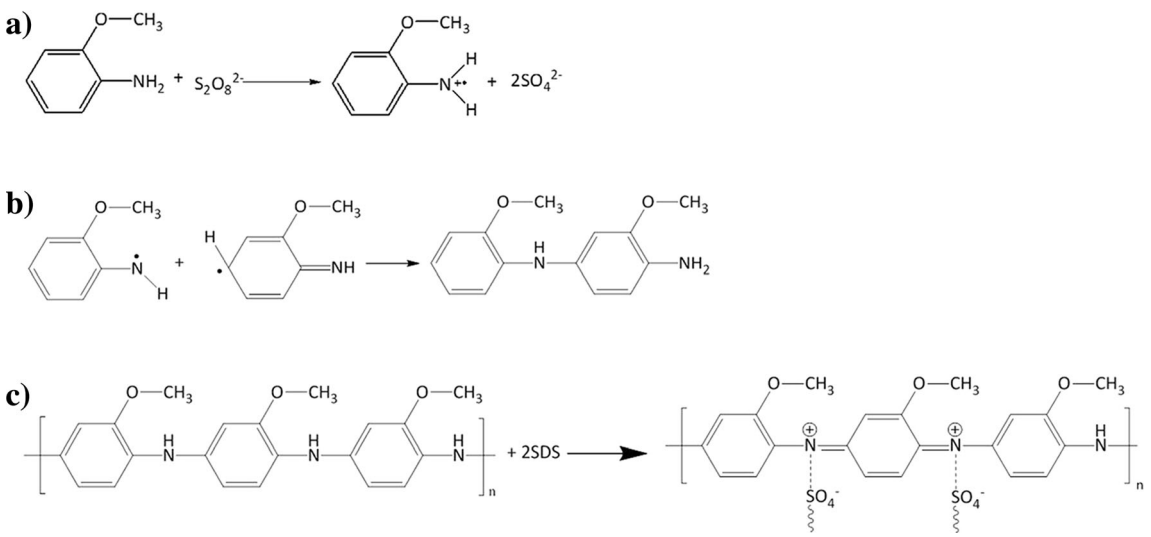

Fig. 1 Proposed polymerization sequences of POA: **a** OA as monomer is oxidized by APS to a cation radical; **b** OA cation radicals form dimers that subsequently get deprotonated; and **c** POA polymer is doped where dodecyl sulfate ion acts as counter ion [12]

DI water, and acetone, then it was dried at 50 °C for 72 h. The code name used in the POA synthesis is POA-time-temperature-SDS mole ratio.

Characterization

The functional groups of POA were investigated by a FT-IR spectrometer (Nicolet, Nexus 670). The FT-IR absorption peaks were taken with 64 scans, at the wavenumber between 400 and 4000 cm^{-1}, and with a resolution of 4 cm^{-1}. The sample was prepared by grinding POA with potassium bromide (dried at 100 °C for 24 h) then compressed to a pellet and inserted in a sample holder.

Proton nuclear magnetic resonance spectroscopy (H-NMR: Bruker, Avance) was used to characterize the functional groups and determine the structure of POA. POA was dissolved in 1 ml of DMSO-d_6 and measured in 30 min to prevent the oxidation of the polymer structure.

The weight loss of volatile molecules, the amount of residual water, and the degradation temperatures of POA were investigated by a TGA analyzer (Perkin Elmer, Pyris Diamond). The samples were weighed in the range of 4–10 mg and loaded into an alumina pan. The thermograms of POA were obtained with a temperature scan from 25 °C to 600 °C at a heating rate of 10 °C/min under nitrogen atmosphere.

The absorption spectra of POA were investigated by UV-VIS absorption spectroscopy (UV-Tecan, Infinite M200) at wavelengths from 230 nm to 1200 nm to identify the POA structure.

The morphology of POA was examined using a scanning electron microscope, SEM, (JEOL, JSM-5410LV). POA particles were placed on a carbon tape and coated with thin layer of gold prior to measurement. Magnifications were 20,000× and 35,000× operating at 15 kV.

Electrical conductivity measurement

Electrical conductivity of POA was measured by a custom-built two-point probe at room temperature and at 60%RH. The sample was compressed into a pellet with a hydraulic compressor. The custom-built two-point probe was connected to a conductivity meter which measured the current that responded to an applied voltage. The specific conductivity (σ) was calculated by using Eq. (1);

$$s = 1/r = 1/(R_s t) = I/(KVt) \quad (1)$$

where, σ is the specific conductivity (S/cm), ρ is the specific resistivity (Ω.cm), R_s is the sheet resistivity (Ω), I is the measured current (A), K is the geometric correction factor as calibrated by using standard silicon wafer sheets with known specific resistivity values, V is the applied voltage (V), and t is the film thickness (cm).

Results and discussion

Characterization

Poly-*o*-anisidine (POA) was synthesized by chemical oxidation polymerization using APS as an oxidant. The polymerization mechanism is shown in Fig. 1. First, the o-anisidine as the monomer is oxidized by APS to form a cation radical (Fig. 1a). The propagation is provided in the second step as shown in Fig. 1b. The interaction of radicals generates the dimer. The polymer formation is created as a result of the recombination of oxidized dimer and initial radical. Finally, the POA is doped by sulfate ion as a counter ion [12].

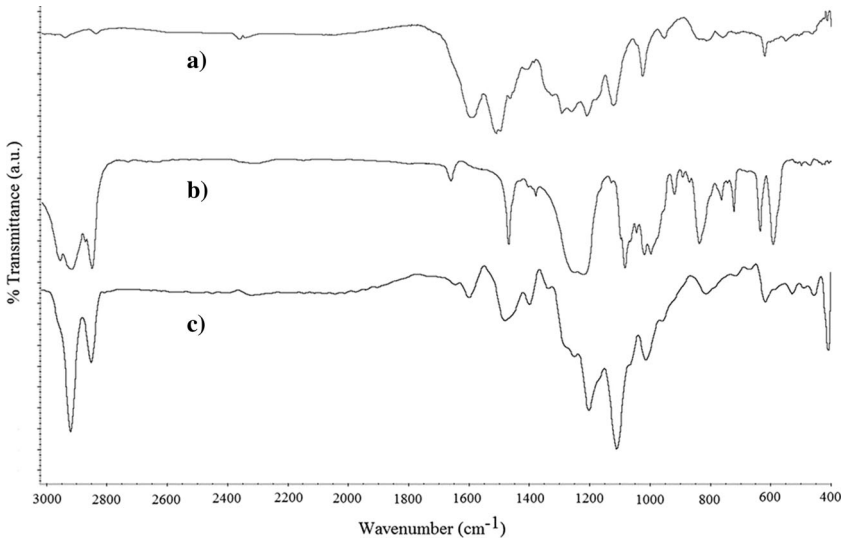

Fig. 2 FTIR spectra of POA: **a** dedoped POA; **b** SDS; and **c** doped POA

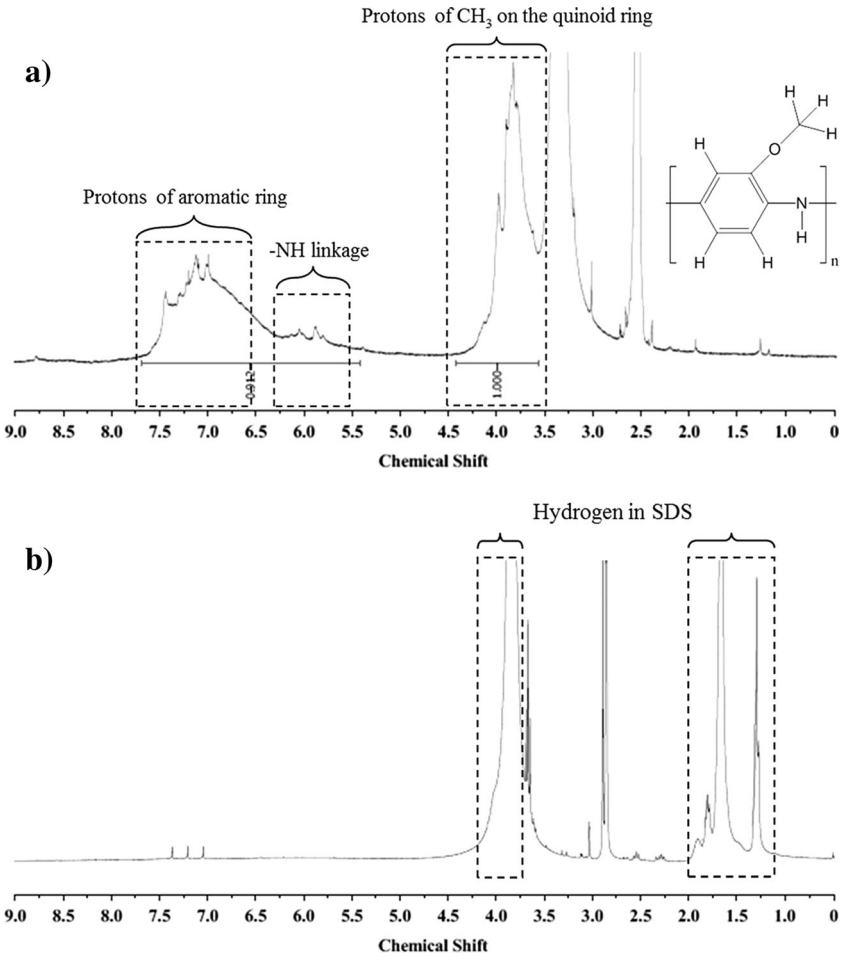

Fig. 3 ^{1}H NMR spectrum of POA: **a** undoped POA and **b** doped POA

The FT-IR spectra of POA are shown in Fig. 2. The peaks at 1579 and 1451 cm^{-1} are characteristics of the C = C stretching of the quinoid and benzenoid rings, respectively [14]. The peaks at 1289,1198, 1166, and 1111 cm^{-1} can be assigned to the C-N^+ stretching, the C-O aromatic stretching, the secondary aromatic amine stretching, and the C-O-C ether group stretching in aromatic ring, respectively [12, 15–17]. Not only characteristic peaks of POA are visible in the FT-IR spectra, but also characteristic peaks of SDS appear which confirm successfully doped POA by SDS. The FT-IR peaks of doped POA are similar to those of the dedoped POA except the peaks at 2928, 1471, 1224, 1087, and 846 cm^{-1} of the former appear which correspond to the C–H stretching and bending, the S = O stretching vibration of SO_4 from SDS molecules, and the C–H stretching, respectively [18].

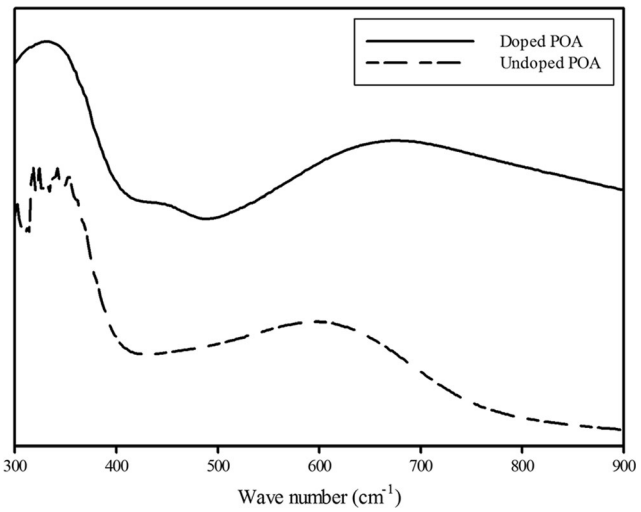

Fig. 4 UV-vis spectra of undoped and doped POA

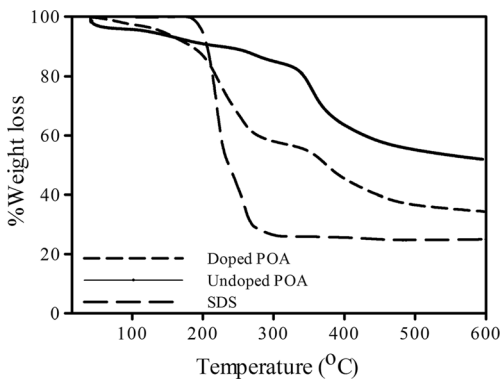

Fig. 5 Thermograms of undoped and doped POA

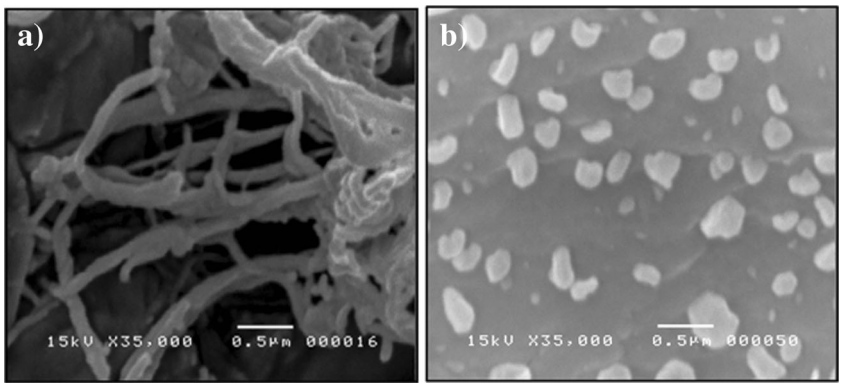

Fig. 6 Morphology of POA nanoparticles prepared using various synthesis temperatures: **a** 3 °C and **b** 25 °C

Figure 3 shows the H-NMR spectra to identify the functional groups and to determine the POA structure. Figures 3a, b display the strong peaks in the region of 2.3–3.5 which can be referred as the protons of DMSO. The POA structure provides the signals in the range of δ = 3.5–4.5 which correspond to the protons of the methyl groups ($-CH_3$) on the quinoid ring. The signals in the range of δ = 6.5–7.5 correspond to the protons of the aromatic rings. The small signals in the region 5.2–6.1 are assigned to the –NH linkages [19, 20]. However, the spectra of doped POA with SDS (Fig. 3b) shows the signal in the range of δ = 1.25–2.0 and δ = 3.8–4.0 corresponding to the interfere peak of proton resonances and $-CH_2$ of SDS, respectively [21].

Figure 4 shows the UV-Vis absorption spectra of doped and undoped POA. The peak at 330 nm observed in both cases corresponds to the bonding to anti-bonding (π-π*) transition of the benzenoid ring [22]. Moreover, the absorption spectrum of doped POA shows the peaks at 430 and 800 nm which are excitations of the polaron due to doping [23]. However, the peak at 800 nm is shifted to 600 nm which can be referred to the POA undoping [23, 24].

The thermal behavior of undoped POA shows two steps of weight loss as shown in Fig. 5. First, the decomposition temperature is 100 °C resulting from the removal of water absorbed in the polymer. Secondly, the decomposition temperature of 350 °C corresponds to the decomposition of POA backbone [14]. In addition, the decomposition temperature of doped POA also exhibits the degradation of dopant (SDS) at 180–250 °C [22]. The degradation of dopant is consistent with the peak of SDS appearing in the FTIR spectra where SDS acts as the dopant on the POA structure as shown in Fig. 1.

Morphology

Effect of polymerization temperature

The morphology of synthesized POA based on the effect of reaction temperatures at 3 °C and 25 °C is shown in Fig. 6. The POA nanoparticles are of nano-fiber shape with the size of 129 ± 33 nm at the polymerization temperature of 3 °C. However, the POA nanoparticles becomes more agglomerated into a non-fiber shape with the size of 322 ± 65 nm at the polymerization temperature of 25 °C. Normally, the polymer particle size decreases with increasing polymerization temperature because the initiator decomposition rate increases with increasing reaction temperature. The increase in initiator decomposition rate leads to inducing a higher nucleation rate or free radical concentration, thus the number of particle increases and the particle size decreases [25–28]. In the present work, the high reaction temperature has an opposite effect here resulting in producing a larger particle than that of lower reaction temperature. This is because the increase in the number of free radicals provides either recombination or other side reaction, such as a chain transfer reaction which causes a decrease in the initiator efficiency resulting in a large particle size [26, 27]. Moreover, the higher reaction temperature also accelerates the polymerization rate and induces the particle agglomeration [29, 30].

Effect of polymerization time

The morphology of POA depends on the polymerization time at polymerization temperature of 3 °C as shown in Fig. 7. The POA nanoparticle is of a fiber shape with the diameter varying

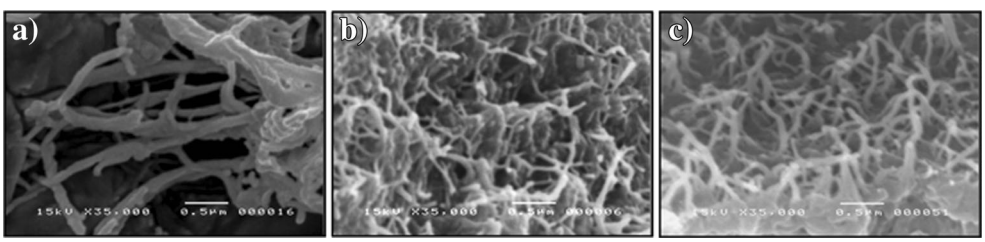

Fig. 7 Morphology of POA nanoparticles prepared using various synthesis times: **a** 18 h; **b** 48 h; and (c) 72 h

from 129 ± 33 nm to 65 ± 8.6 nm. The POA nanoparticle size decreases with increasing polymerization time, from 129 ± 33 nm to 65 ± 8.6 nm for 18 and 48 h, respectively. The POA synthesized for 18 h is of the largest size in an incomplete fiber form because the shorter polymerization time provides the incomplete polymerization of POA [31]. With increasing reaction time, the free radical concentration in the system increases resulting in increasing amount of POA polymer chain and a full POA nano-fiber form [32]. Thus, the polymerization time of 48 h provides the smallest POA nanoparticle in the full fiber form. However, the POA nanoparticle becomes of a larger fiber size when POA is synthesized for 72 h (POA nanoparticle size of 75 ± 14 nm). With polymerization time progress, the polymer can grow to a longer chain length because of more time to induce chain propagation which provides a larger particle size. Moreover, there is more time to induce polymer chain reaction together to connect and terminate polymer chain with, resulting in particle agglomeration and a larger size [29, 33].

Effect of SDS concentration

The particles size of synthesized POA under the effect of SDS concentration at 3 °C for 48 h varies between 65 ± 8.6 nm and 90 ± 18 nm and the particles shape varies from non-uniformed shapes to a nanofiber at the 0.008 to 10.00 mol ratios of SDS/OA, as shown in Fig. 8. The SDS amount that is suitable to produce POA into the full-nanofiber is at the SDS/OA mole ratio of 8.00, with the diameter of 65 ± 8.6 nm. At the SDS/OA mole ratio of 0.008, the POA particle is the largest in non-uniformed shapes because SDS concentration is lower than that of CMC (CMC of SDS is at the SDS/OA mole ratio of 0.12) and thus no micelle occurs for supporting polymerization. At SDS concentration higher than CMC, POA forms a fiber shape due to the packing parameter effect. The packing parameter ($V_H/l_c a_0$) is used to identify the micelle shape. The packing parameter of SDS is ~0.32 which provides the cylindrical shape of micelle (cylindrical micelle is obtained from packing parameter in the range of 0.3–0.5) [35]. The POA fiber becomes more agglomerated when the SDS/OA mole ratio is 12:00. At a higher SDS concentration, the amount of micelle increases and induces more micelle fusion resulting in the POA particle agglomeration [34].

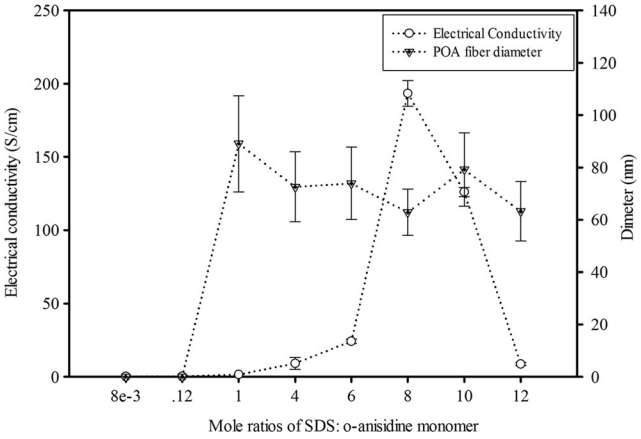

Fig. 9 Electrical conductivity and fiber diameter of poly *o*-anisidine at various mole ratios of SDS: *o*-anisidine monomer

Electrical conductivity

The electrical conductivity increases from 8.8×10^{-2} S/cm to 168.96 S/cm with increasing SDS/OA mole ratio as shown in

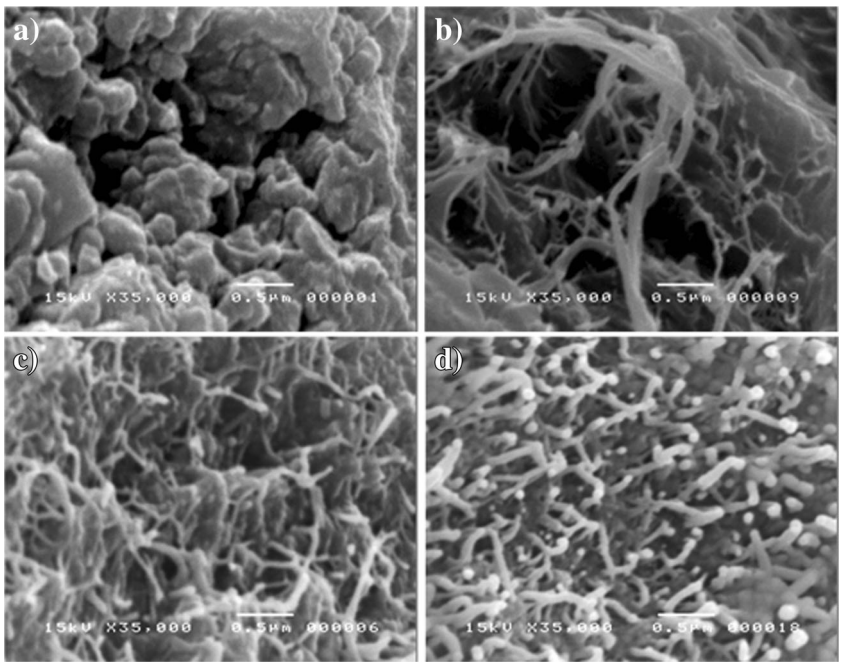

Fig. 8 Morphology of POA nanoparticles prepared using various SDS mole ratios: **a** 0.008; **b** 4.00; **c** 8.00; and **d** 10.00

Fig. 9. At the SDS mole ratio of 8.00, the highest conductivity of 168.96 S/cm is obtained. The SDS can act also as a dopant resulting in increasing doping level with increasing SDS concentration [34, 36]. The SDS consists of an anion of sulfate group, it can induce the structure of POA to attain more conjugated double bonds. However, the electrical conductivity decreases when the SDS mole ratio is higher than 8.00 because the reaction of self-screening occurs during the polymerizing and doping by SDS anions which provides an over-oxidation process [34]. Moreover, the electrical conductivity not only depends on doping level but also depends on morphology. The magnitude of the highest electrical conductivity obtained is 168.96 S/cm at the SDS/OA mole ratio of 8.00. This ratio provides the full fiber morphology (with a diameter of 65 ± 8.6 nm) with the highest electrical conductivity (168.96 S/cm) because of the higher surface area for electrons to transfer [34]. One of the mechanisms of the electrical conductivity based on the effects of particle size and shape is the inter-particle conductivity. The inter-particle conductivity is related to the connectivity by direct contact (Ohmic) among particles. A smaller particle size provides more efficiently conductive networks than a larger particle size due to a higher surface area resulting in a greater charge transport and a higher electrical conductivity. Moreover, the electrical conductivity is influenced by the particle shape. If a particle shape has a greater conductive contact area of neighboring particles, it provides a greater charge transfer and promote a higher electrical conductivity. Thus, the fully fiber shape is a better connection with neighboring particles than other particle shapes, and it provides a higher electrical conductivity [37, 38].

Previously, POA was synthesized in the rod-shape with the size of 40–50 nm by using SDS as a surfactant because SDS created the cylindrical micelle as reported by Jadhav et al. [39]. Moreover, POA was also synthesized by chemical oxidation polymerization at various dopants as methane sulfonic acid (MSA), hydrochloric acid (HCl), and p-toluene sulfonic acid (pTSA). The type of dopants affected the POA shape and the electrical conductivity. The pTSA provided the highest electrical conductivity when compared with HCl and MSA because the molecular structure of pTSA could stabilize the bond between the dopant and the polymer chain through the benzene ring of the dopant anion resulting in the formation of a resonance structure for electrons to flow over the entire polymer chain [40].

To confirm the best POA properties, the POA synthesis at the condition of 48 h, 3 °C, and 8 mol ratio of SDS: *o*-anisidine monomer was repeated. The POA particles were reproduced in which electrical conductivity obtained was 144.47 ± 72.83 S/cm. The POA characteristics namely chemical properties (FT-IR, UV-vis, H^1-NMR), thermal properties (TGA), and morphology (cylindrical shape, 77 ± 17.7 nm) were also remeasured and nearly the same results were obtained.

Thus, the morphology and electrical conductivity of POA depend on the polymerization conditions such as temperature and time of polymerization, surfactant concentration, and characteristics of dopant. In addition, the electrical conductivity is critically dependent on the morphology and particle size of POA.

Conclusion

In the present study, POA nanoparticles were successfully synthesized using APS as an oxidant and SDS as a surfactant platform in the chemical oxidation polymerization. The particle size varied in the range of 63 to 129 nm depending on the polymerization temperature, polymerization time, and SDS concentration. These synthesis conditions produced POA nanofibers. The POA nanofiber size increased with increasing polymerization time and SDS concentration because these factors controlled the polymerization rate and induced particle agglomeration and particle connection. The electrical conductivity of POA increased from 0.025 to 168.96 S/cm with decreasing POA nanoparticle size. The synthesis condition that generated the highest electrical conductivity (168.96 S/cm) with connected nano-fiber (65 ± 8.6 nm) was the POA synthesized using 8:00 mol ratio of SDS at 3 °C for 48 h.

Acknowledgments The authors would like to acknowledge the Conductive and Electroactive Polymers Research Unit of Chulalongkorn University, the Thailand Research Fund (TRF), and the Royal Thai Government for the financial supports.

References

1. Dai L (2004) Intelligent macromolecules. Intelligent Macromolecules for Smart Devices Springer London: 81–116
2. Balint R, Cassidy N, Cartmell SH (2014) Conductive polymer: Towards a smart biomaterial for tissue engineering. Acta Biomareialia 10:2341–2353
3. Molapo KM, Ndangili PM, Ajayi RF, Mbambisa G, Mailu SM, Njomo N, Masikini M, Baker P, Iwuoha E (2012) Electronics of conjugated polymers (I): polyaniline. Int J Electrochem Sci 7: 11859–11875
4. Ozyilmaz AT, Ozyilmaz G, Yigitoglu O (2010) Synthesis and characterization of poly(aniline) and poly(o-anisidine) films in sulphamic acid solution and their anticorrosion properties. Prog Org Coat 67:28–37
5. Tatyana VV, Oleg NE (1997) Polypyrrole: a conducting polymer; its synthesis, properties and applications. Russ Chem Rev 66:443
6. Shirakawa H, Louis EJ, MacDiarmid AG, Chiang CK, Heeger AJ (1977) Synthesis of electrically conducting organic polymers: halogen derivatives of polyacetylene, (CH. J Chem Soc Chem Commun 16:578–580
7. Wankhede MG, Koinkar PM, More MA, Patil PP, Gangal SA (2002) Synthesis of poly(o-anisidine) coatings on low carbon steel by electrochemical polymerization of o-anisidine. Adv Polym Technol 21:33–43

8. Mazrouaa AM, Abed MY, Mansour NA, Mohamed MG (2012) Synthesis and characterization of poly o-anisidine nanoparticles and their nanocomposite. Mater Sci Eng 1:1–5
9. Valentini L, Bavastrello V, Stura E, Armentano I, Nicolini C, Kenny JM (2004) Sensors for inorganic vapor detection based on carbon nanotubes and poly(o-anisidine) nanocomposite material. Chem Phys Lett 383:617–622
10. Chaudhari S, Patil PP (2007) Corrosion-protection aspects of electrochemically synthesized poly(o-anisidine) coatings on mild steel: an electrochemical impedance spectroscopy study. J Appl Polym Sci 106:400–410
11. Chen ZK, Ng SC, Li SFY, Zhong L, Xu L, Chan HSO (1997) The fabrication and evaluation of a vapour sensor based on quartz crystal microbalance coated with poly(o-anisidine) langmuir–Blodgett layers. Synth Met 87:201–204
12. Khan AA, Habiba U, Khan A (2009) Synthesis and characterization of organic-inorganic nanocomposite poly-o-anisidine Sn(IV) arsenophosphate: Its analytical applications as Pb(II) ion-selective membrane electrode. IntJ Anal Chem 2009:1–10
13. Brüggemann B, Organero JA, Pascher T, Pullerits T, Yartsev A (2006) Control of electron transfer pathways in a dye-sensitized solar cell. Phys Rev Lett 97:208301
14. Mondal RA, Dongre SP, Mahatme UB, Tabhane VA, Hedau MJ. Kondawar SB (2006) Studies on chemically synthesized doped poly(o-anisidine) and copoly{aniline-(o-anisidine)}. Mod Phys Lett B 20:1461–1470
15. Khan AA, Shaheen S, Habiba U (2012) Synthesis and characterization of poly-o-anisidine Sn(IV) tungstate: a new and novel organic inorganic nano-composite material and its electro-analytical applications as Hg(II) ion-selective membrane electrode. J Adv Res 3: 269–278
16. Pandey SS, Annapoorni S, Malhotra BD (1993) Synthesis and characterization of poly(aniline-co-o-anisidine). A processable conducting copolymer. Macromolecules 26:3190–3193
17. Wang G, Wang L, Li X (2005) Synthesis and characterization of poly(o-anisidine)/V2O5 and poly(o-anthranilic acid)/V2O5 nanocomposites. Polym Int 54:1082–1087
18. Ramimoghadam D, Hussein MZ, Taufiq-Yap YH (2012) The effect of sodium dodecyl sulfate (SDS) and cetyltrimethylammonium bromide (CTAB) on the properties of ZnO synthesized by hydrothermal method. Int J Mol Sci 13:13275–13293
19. Raotole PM, Koinkar P, Joshi B, Patil SR (2015) Corrosion protective poly(aniline-co-*o*-anisidine) coatings on mild steel. J Coat Technol Res 12:757–766
20. Valle MA, Gacitua MA, Borrego ED, Zamora PP, Diaz FR, Camarada MB, Antilen MP, Soto JP (2012) Electro-synthesis and characterization of aniline and *o*-anisidine oligomers. Int J Electrochem Sci 7:2552–2565
21. Hassan PA, Raghavan SR, Kaler EW (2002) Microstructural changes in SDS micelles induced by hydrotropic salt. Langmuir 18:2543–2548
22. Kulkarni MV, Viswanath AK, Khanna PK (2006) Synthesis and characterization of poly(o-anisidine) doped with polymeric acids. Int J Polym Mater 55:501–512
23. Yang C, Fang Z, Zhang P (1999) UV-Vis spectra of polyaniline doped with camphor sulfonic acid in different organic solvents. J Cent S Univ Technol 6:127–129
24. Patil S, Mahajan JR, More MA, Patil PP, Gosavi SW, Gangal SA (1998) Electrochemical polymerization of poly(o-anisidine) thin films: effect of synthesis temperature studied by cyclic voltammetry. Polym Int 46:99–105
25. Abdollahi M, Yousefi MR, Alamdari P, Ranjbar H, Najafi FS, Rekabdar F (2013) Synthesis of polybutadiene nanoparticles via emulsion polymerization: effect of reation temperature on the polymer microstructure, particle size and reaction kinetics. Journal of oil, gas and petrochemical. Technology 1:1–16
26. Suppaibulsuk B, Rempel GL, Prasassarakich P (2011) Synthesis of styrene-g-polyisopren nanoparticles by emulsion polymerization and its effect on properties of polyisoprene composites. Polym Adv Technol 13:1473–1483
27. Tanrisever T, Okay O, Sonmezoglu IC (1998) Kinetics of emulsifier-free emulsion polymerization of methyl methacrylate. J Appl Polym Sci 61:485–493
28. Wu G, Wang C, Tan Z, Zhang H (2011) Effect of temperature on emulsion polymerization of n-butyl acrylate. Prod Eng 18:353–357
29. Boguslavsky L, Baruch S, Margel S (2005) Synthesis and characterization of polyacrylonitrile nanoparticles by dispersion/emulsion polymerization process. J Colloid Interface Sci 289:71–85
30. Huajing Z, Yadong J, Jianhua X, Yajie Y (2010) The characteristic properties of PEDOT nano-particle based on reversed micelle method. Sci China Technol Sc 53:2355–2362
31. Parvole J, Ahrens L, Blas H, Vinas J, Boissiere C, Sanchez C, Save M, Charleux B (2010) Grafting polymer chains bearing an N-succinimidyl activated ester end-group onto primary amine-coated silica particles and application of a simple, one step approach via nitroxide-mediated controlled/living free-radical polymerization. J Polym Sci A Polym Chem 48:173–185
32. Mohy Eldin MS, Elaassar MR, Elzatahry AA, Al-Sabah MMB (2014) Poly(acrylonitrile-co-methyl methacrylate nanoparticles: I. Preparation and characterization Arabian J Chem doi:10.1016/j.arabjc.2014.10.037
33. Lee JM, Kang SJ, Park SJ (2009) Synthesis of polyacrylonitrile based nanoparticles via aqueous dispersion polymerization. Macromol Res 17:817–820
34. Paradee N, Sirivat A (2014) Synthesis of poly(3,4-ethylenedioxythiophene) nanoparticles via chemical oxidation polymerization. Polym Int 63:106–113
35. Rosen MJ (2004) Micelle formation by surfactants. Surfactants and interfacial phenomena, John Wiley & Sons, Inc 105–177
36. Tadros TF (2009) Applied surfactants principles and applications: Physical chemistry of surfactant solutions. Wiley-VCH Verlag GmbH & Co. KGa, pp 19–40 doi:10.1002/3527604812.ch2
37. Kline RJ, McGehee MD (2006) Morphology and charge transport in conjugated polymers. J Macromol Sci Polym Rev 46:27–45
38. Heo SI, Yun JC, KS O, Han KS (2006) Influence of particle size and shape on electrical and mechanical properties of graphite reinforced conductive polymer composites for the bipolar plate of PEM fuel cells. Adv composite. Mater 15:115–126
39. Jadhav RS, Hundiwale DG, Mahulikar PP (2010) Synthesis of nano polyaniline and poly-o-anisidine and applications in alkyd paint formulation to enhance the corrosion resistivity of mild steel. J Coat Technol Res 7:449–454
40. Wang X, Ray S, Gizdavic-Nikolaidis M, Easteal AJ (2011) The effects of dopant acids on structure and properties of poly(o-methoxyaniline. J Polym Sci A Polym Chem 50:353–361